Near-infrared modeling and enhanced visualization, as a novel approach for 3D decay mapping of stone sculptures

This is a post-peer-review, pre-copyedit version of an article published in *Archaeological and Anthropological Sciences*. The final authenticated version is available online at: https://doi.org/10.1007/s12520-020-01110-5

ORIGINAL PAPER

Near-infrared modeling and enhanced visualization, as a novel approach for 3D decay mapping of stone sculptures

Efstathios Adamopoulos

Department of Computer Science, Università Degli Studi di Torino, Corso Svizzera 185, 10149 Torino (TO), Italy

ORCID iD: 0000-0003-4358-474X

Fulvio Rinaudo

Department of Architecture and Design, Politecnico di Torino, Viale Mattioli 39, 10125 Torino (TO), Italy

ORCID iD: 0000-0002-9592-1341

Corresponding author: Efstathios Adamopoulos efstathios.adamopoulos@unito.it

Acknowledgments

The authors would like to acknowledge *Musei Reali Torino* and *Ragione Piemonte* for the courteous concession of permission to publish the results about the statue from the Fountain of Hercules, and the sculpture of Christ Crucified respectively. Furthermore, the authors would like to acknowledge the contribution of Alessandro Bovero for his useful advice, Marie Claire Canepa coordinator of the Lab for Mural Paintings, Stonework And Architectural Surfaces at *Fondazione Centro Conservazione e Restauro dei Beni Culturali 'La Venaria Reale'* for facilitating the data acquisition for the statues, and Dr. Stefania De Blasi and Marianna Ferrero at the Dept. of Programming and Development at *Fondazione Centro Conservazione e Restauro dei Beni Culturali 'La Venaria Reale'* for making possible the publishing of the results produced at the labs of the conservation and restoration center mentioned above, outside of Turin.

Abstract

Representation of the surface pathology of heritage objects imposes a problematic task. It usually involves the implementation of on-site visual inspections, diagnostic procedures on-site, and after sampling, through minimally destructive laboratory tests, to produce area-specific results or two-dimensional mapping visualizations. Mapping of stone weathering is usually performed manually with time-consuming two-dimensional approaches, thus losing the importance of topology and, in general, its three-dimensional metric quality. The recent introduction of modified cameras to heritage science has enabled enhanced observation at higher resolutions, concomitantly having the capacity to produce datasets that can be used for direct image-based three-dimensional reconstruction. With this article, we present a novel work combining near-infrared imaging using a modified sensor, and contemporary dense multiple-image reconstruction software, to produce spectral models of historical stone sculptures. This combined approach enables the simultaneous capturing of the shape of the historical stone surfaces and the different responses of deteriorated materials in the near-infrared spectrum. Thus, we investigate the capacity of the suggested method to assist three-dimensional diagnosis and mapping of stone weathering. We explore the usability of produced spectral textures via classification, and three-dimensional segmentation techniques to obtain and assess different types of visualization. We additionally evaluate the produced models for their metric and radiometric properties, by comparing them with models produced with visible spectrum imagery, acquired with similar capturing parameters.

Keywords:

Near-infrared imaging; Modified camera; Multi-view image recording; Decay mapping; Heritage diagnostics

Introduction and background

Innovative methods for documenting and visualizing the state of preservation of heritage objects, and especially of those exposed in external environments, are becoming increasingly important. This heightened interest stems from an increasing need to ensure the sustainability of tangible heritage, and therefore devise novel low-cost, easily implementable, and repeatable solutions applied for rapid diagnostics. The definition and modeling of the three-dimensional (3D) geometry and the deterioration patterns for historical stone objects, constitute crucial steps towards ensuring their safeguarding from environmental influences. If accurately carried out, they can effectively assist the planning of conservation interventions and long-term preservation strategies. Contemporary approaches typically follow separate workflows for the heritage 3D recording, diagnostics, and decay mapping of stone

sculptures, employing vastly different instrumentation and computational procedures. Before discussing the integrative approaches for the above, we should, therefore, briefly review each technique individually.

Multi-view 3D reconstruction

Multi-view image recording refers to reconstruction approaches similar to conventional photogrammetry, for the generation of 3D point clouds and models from overlapping images, using robust automated algorithms (Fonstad et al. 2013; Koutsoudis et al. 2014). Standard multi-view reconstruction pipelines start with detection and description on every image of a dataset. Then follow Structure-from-Motion (SfM) implementations to estimate the camera positions and 3D point coordinates in a local coordinate system without a real scale, producing a sparse cloud. Subsequently, the 3D point cloud is further densified by employing dense image matching algorithms, and most pixels of the scene are reconstructed in a procedure typically called Multiple-View-Stereo (MVS). Later the dense point cloud is meshed into a 3D model, usually using triangulation algorithms, and textured by interpolating color information from the imagery dataset. Multi-view recording approaches do not require the implementation of control points with known coordinates. However, the use of control points during the orientation improves the accuracy of the results and is mandatory for geo-referencing. For applications oriented towards digital visualization referencing, or scaling is not mandatory, as for applications that require metric 3D products.

Multi-view image recording techniques constitute cost-effective alternatives to traditional close-range photogrammetry, which can effectively involve oblique imagery from consumer-grade cameras, to produce accurate and high-resolution spatial results (Hassani 2015; Georgopoulos and Stathopoulou 2017). In addition, they require low levels of supervision and user-expertise. As a result, these techniques have become widely used in heritage science. Typical applications involve the documentation of archaeological remains (McCarthy 2014; Douglass et al. 2015; López et al. 2016; Toprak et al. 2019), architectural details (Columbu and Verdiani 2014; Tucci et al. 2015; Russo et al. 2019), sculptures (Malik and Guidi 2018; Girelli et al. 2019; Koehl and Fuchs 2019), artifacts (Santos et al. 2017; Adamopoulos and Rinaudo 2019), implementations to support the integration of multi-disciplinary diagnostical data (Adamopoulos et al. 2017; Mandelli et al. 2017), and virtual restorations or reconstructions (Tucci et al. 2017; Chen et al. 2018; Fazio and Lo Brutto 2020).

Assessing the state of conservation

Stone surfaces exposed to external environments constitute substrates where microorganisms can adhere, and depending on the material bio-receptivity, grow accordingly. They play a crucial role in the development of

aesthetic and physicochemical alterations exerting destructive mechanical forces and causing chemical degradations in the stone material. It is estimated that biological weathering can be even severer than the non-biogenic degradation, representing a serious cause of deterioration of the outdoor stone cultural heritage all over the world (Tiano 2002; Nascimbene and Salvadori, 2008; Marvasi et al. 2012). Therefore, diagnostics of the bio-deterioration patterns are essential towards the conservation and preservation works of historical stone sculptures.

The diagnostical studies to assess the state of preservation of historical stone surfaces typically involve interpretation, analysis, recording, and quantification of the degradation patterns, taking into account all geometrical characteristics, historical data of the construction, properties of the materials, environmental factors, and on-site observations (Fitzner 2002; Kioussi et al. 2013). If deemed necessary, based on the above results, specific representative areas are selected for more in-depth investigations, with laboratory non-destructive testing and evaluation techniques, after sampling (Dumas et al. 2004; Mascalchi et al. 2017). Both the on-site and in-lab instrumental diagnostic studies help a thorough understanding of the development and mechanisms of decay. An important method towards visualizing the decay products, selecting areas of interest for sampling, and decision making for conservation and protection, is mapping the materials and decay.

Mapping the state of conservation

Mapping of historical stone surfaces is a method that has been well established between non-destructive procedures, used for accurate documentation, diagnosis, and assessment of stone materials and relevant degradation phenomena. This method is applicable for all stone materials, and the results can be analyzed through computational systems and commonly spatial information systems to acquire useful conclusions with geometrical substance. Digitized spatial information (spatial entities) of the deterioration, which have geometric attributes and are geo-referenced, can be correlated to each other and thus compared spatially. This digitization enables us to ask synthesized questions, to visualize and calculate statistical data, and to perform quantitative evaluations (Fitzner 2004). Traditionally two-dimensional (2D) mapping of the scales of stone weathering has been performed with computer-assisted design (CAD), and geographical information systems (GIS) platforms, or combination of both, for photographs or orthophoto-maps (Inkpen et al. 2001; Salonia and Negri 2003; McCabe et al. 2007; Delegou et al. 2013). More recently, after the introduction of 3D laser scanning and multi-view 3D reconstruction, direct mapping on high-resolution 3D models has been explored with specialized software (Siedler and Vetter 2013; Ansel et al. 2016; Kozub and Kozub 2016), programs for editing 3D models (Pfeuffer et al. 2018) through

segmentation of areas with different damage levels, 3D GIS software (Campanaro et al. 2016), and web-based implementations (Apollonio et al. 2018). It should be highlighted that most of the relevant research refers to manually mapping different forms or levels of weathering, a highly time-consuming task. More automated approaches have been explored through 2D digital processing of visible images (Vázquez et al. 2011; Moropoulou et al. 2013; Ortiz et al. 2017) and exploiting intensities detected through laser scanning (Chrysostomou et al. 2010; Suchocki 2020); although most of these applications refer mostly to building-scale implementation.

Near-infrared imaging

Near-infrared (NIR) imaging is a specialized photography technique which has been highly associated with archaeological investigations, mainly regarding the polychromy of paintings (Delaney et al. 2016; Vandivere et al. 2019) and sculptures (Sfarra et al. 2014; Gasanova et al. 2018). NIR imaging has also been explored to recognize corrosion on stone architectural heritage (Lerma et al. 2000; Lerma et al. 2012), and bronze sculptures (Catelli et al. 2018). The recent introduction of digital cameras employing CCD (charge-coupled device) and CMOS (complementary metal–oxide–semiconductor) sensors, modified for near-infrared or full-spectrum imaging (coupled with external NIR filters) has made high-resolution NIR imaging more feasible. These modified sensors constitute a low-cost solution, which retains user-friendly features and interfaces to a wide variety of photographic accessories and software (Webb et al. 2018; Pronti et al. 2019). Contemporary research (Adamopoulos et al. 2019; Adamopoulos and Rinaudo 2020), which shows promising results regarding the combination of NIR imaging and multi-view 3D reconstruction for heritage-oriented applications, led us to the motivation for this research.

Methodological approach

The presented research draws motivation from the above, thus aiming to suggest and evaluate an approach for the simultaneous recording of geometrical features and state-of-preservation-related characteristics of historical objects, exposed under environmental pressures. In this work, we combine NIR imaging performed with a modified commercial camera, image-based multi-view 3D modeling, and 3D mapping techniques. We aim to explore a low-cost, rapid, and easily implementable method for diagnostics of stone heritage. Towards this direction, we produce NIR spectral models using two algorithmic implementations and evaluate their metric quality. We further discuss the geometric results in comparison to models produced by visible (VIS) spectrum imagery. Then we use the high-quality NIR models produced to implement different mapping techniques based on classification and segmentation approaches, exploiting the high-resolution NIR intensities to produce different visualizations. Afterward, we assess

the 3D visualization results on the capacity to represent the levels of weathering on historical stone sculptures accurately. Aiming to evaluate the applicability of the suggested method on different scales, we implement it for two case studies of different dimensions.

Materials and algorithms

Case studies

To evaluate the suggested approach on different scales, two different case studies of historical stone sculptures exposed to external environmental conditions were involved. The first one was a 17th-century marble statue (approx. height 1.75 m) from the Fountain of Hercules at the *Reggia di Venaria Reale* near Turin. The Palace of *Venaria* was one of the Residences of the Royal House of Savoy, included in the UNESCO World Heritage List in 1997. *Musei Reali Torino* owns the statue. The second case study was a small 19th-century religious stone sculpture of Christ crucified (approx. dimensions 31 cm × 22 cm) from *Castello di Casotto* (Garessio, Province of Cuneo, Piedmont) owned by *Regione Piemonte*. The *Casotto* Castle was originally a Carthusian monastery, later acquired by the Savoy and transformed into a castle and hunting lodge by Carlo Alberto (see Fig. 1).

Fig. 1 Images of the case studies; statue from the Fountain of Hercules (left) and small stone sculpture of Christ Crucified (right)

Equipment

For this work, the images were captured with a low-cost (500$) Digital Single-Lens Reflex (DSLR) camera. The utilized Canon Rebel SL1, converted for full spectrum acquisition by 'LifePixel Infrared', employs an 18.0 MP APS-C CMOS sensor (22.3 × 14.9 mm^2, 4.38 μm pixel size), with 14-bit DIGIC 5 processor. NIR image acquisition was

performed with the implementation of a near-infrared-pass filter (700–1400 nm), and VIS image acquisition was performed with the implementation of a UV-NIR-cut filter. Additionally, a Canon EF-S 18–55 mm f/4–5.6 IS II zoom lens was used. To avoid micro-movement effects, the camera was mounted on a tripod during all acquisition scenarios. An x·rite ColorChecker® Classic with 24 colors was used for color balancing, utilizing middle gray for visible white-balancing and foliage green for the near-infrared color-balancing. Post capturing photo-editing operations were performed in Adobe Lightroom Classic.

Software and hardware

Multi-view image-based 3D reconstructions were conducted with Agisoft Metashape Professional (AMP) 1.5.1 and with 3DFlow Zephyr Aerial (FZA) 4.519. Both software is based on Structure-from-Motion (SfM), and Multiple-View-Stereo (MVS) approaches. AMP employs scale-invariant feature transform (SIFT)-like detection and description, then calculates approximate relative camera location and used Global bundle-adjustment to refine them, a type of MVS disparity calculation for dense reconstruction and Screened Poisson surface reconstruction. FZA employs a modified Difference-of-Gaussian (DoG) detector, a combination of Approximate Nearest Neighbor Searching, M-estimator Sample Consensus and Geometric Robust Information Criterion for matching, then hierarchical SfM and Incremental adjustment, dense MVS reconstruction with fast visibility integration, tight disparity bounding and finally meshing with an edge-preserving algorithmic approach was selected to differentiate from AMP. To be able to compare the performance between the two different algorithmic implementations with NIR datasets, we attempted to employ similar photogrammetric reconstruction parameters inside both software, when applicable.

Metrical comparisons and manipulation of the final textured models were performed with the open-source software Cloud Compare. Segmentation of the NIR textured models to create 3D thematic mapping was performed in free and open-source software MeshLab (Callieri et al. 2013). The 3D visualizations were realized in the free software Cloud Compare. All image-based processing was performed with the same laptop, with a Hexa-core Intel i7-8750H CPU at 2.2 GHz (Max 4.1 GHz), 32 GB RAM, and an NVIDIA GeForce RTX2070 GPU.

Application

Data acquisition

The dense capturing of the images was planned according to the software manuals and considering relevant works with similar algorithmic implementations. For both case studies, rigid imagery datasets were acquired, with large overlaps (over 80%), from close ranges (Fig. 2). We attempted to maintain constant the internal and external capturing parameters, as well as the ground sampling distances (GSD) between the NIR and VIS spectra, to increase the comparability of the final 3D models. In this way, we facilitated both the metric evaluations and the assessment of the performance of SfM/MVS based reconstruction from NIR images.

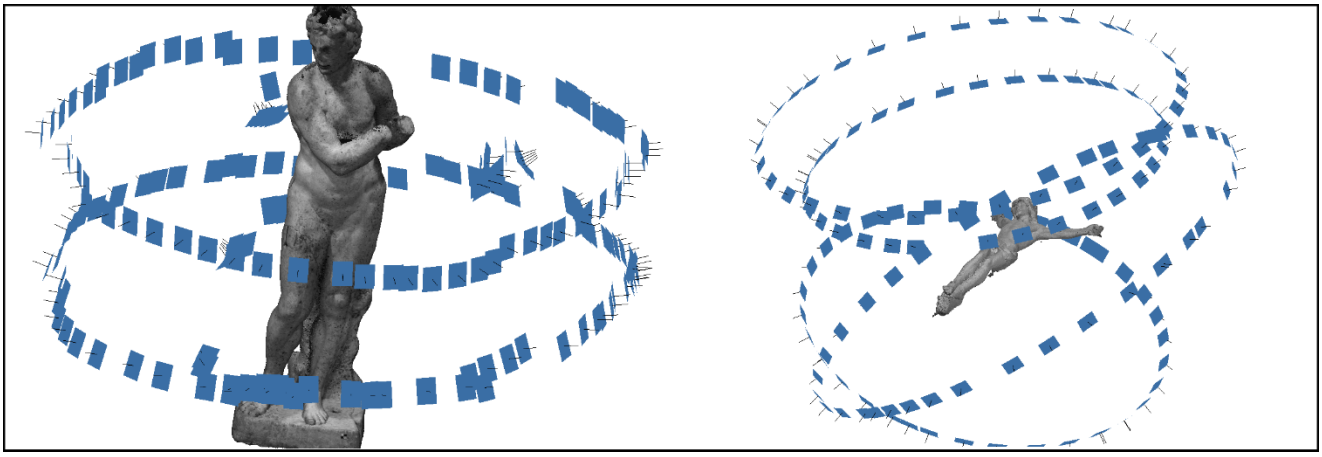

Fig 2. Image capturing scenarios; statue from the Fountain of Hercules (left) and small stone sculpture of Christ Crucified (right)

We used low ISO values to prevent sensor luminance noise, simultaneously maintaining the exposure durations under the clipping limit value. The images were captured in Canon's raw image format (.cr2) to avoid the loss of valuable intensity data. We selected 180 images for the first case study and 142 for the second, for each spectrum. We summarize the capturing conditions used to collect the datasets in Table 1. It should be highlighted that for the first case study, we did not use flash as it resulted in extremely variable light conditions due to the geometry of the sculpture and the non-uniform illumination by various light sources inside the conservation labs where it was hosted. Also, we were not able to implement the same camera positions for VIS and NIR imaging, but we marked and maintained a constant distance from the object and similar angles between each position. For the case study of the Crist Crucified sculpture, we used a ring flash and were able to eliminate all shadows in a more controlled environment. The images of different spectra were captured from the same positions. Additionally, for this case study, we utilized a turntable during acquisition and rotated the object four times to capture different but overlapping

sides. Scaling for the first case study was performed by using an invar scale bar of 1.000165m (±15 nm). Additionally, small paper targets were placed at the base and the body of the marble statue to assist the orientation between the 3D models. The scaling of the second case study was performed by using as reference the measured dimensions of the wooden cross (precision of measuring ±0.25 mm)

Table 1 Characteristics of the imagery datasets

Case study	f [mm]	Distance [cm]	GSD [mm]	Spectrum	f-stop	Exposure [s]	ISO
1	18.0	98	0.22	VIS	f/11	1/2	200
1	18.0	98	0.22	NIR	f/11	5	200
2	18.0	38	0.09	VIS	f/16	1/15	100
2	18.0	38	0.09	NIR	f/16	1/15	100

Image pre-processing

Before processing, raw VIS images of the marble statue were digitally manipulated to soften the highlights and the shadows, as this was later resulting in high surface noise on the 3D models, paying attention to not eliminate the surface features useful for image-based modeling. NIR images were exported in a single-band format, and were not further manipulate to not compromise captured NIR intensities In addition to that, all the implemented images were masked accordingly in both software, to exclude the unwanted areas of each scene, and out-of-focus areas, to increase the quality of imagery, therefore reducing noise levels and processing times.

Image-based 3D digitization

Multi-view image reconstructions with NIR and VIS imagery followed a standard semi-automatic SfM/MVS pipeline, similar in both software despite the significant differences in algorithmic implementations. We used similar reconstruction parameters between them, regarding volumes and quality of processing outputs (max. of 10M triangles for the meshes). The 3D models were constructed in a four-step procedure. The first step referred to the sparse reconstruction of each object, with a concurrent estimated calculation of the cameras' relative orientation, and autocalibration with SfM approaches. For this step, the chosen accuracy and density parameters were the highest available in both software. The sparse point clouds were filtered from noise according to re-projection errors, and local cluster distances with statistical filtering. For the second step, results were densified by employing MVS stereo-matching algorithms. The third step comprised of meshing the dense point clouds into triangular surfaces (Delaunay algorithm). The generated meshes were subsequently cleaned from small unconnected components and spikes. The final step involved the application of texture mapping to acquire single-file high-

resolution textures from the original images. Given the high quality of original imagery, we constrained color balancing and blending between images to reduce the possibility of radiometric errors. When choosing the resolution of textures, we considered sampling distances to be at least two or three times higher than the original pixel sizes. Between each stage of the reconstructions, we performed thorough visual checks to determine quality, and then we followed de-noising procedures, identically for all the produced dense results, to not reduce comparability.

Mapping the surface weathering

The 3D mapping was accomplished with two alternative procedures to enhance NIR modeling results towards an accurate visualization of the surface pathology. It was performed based on the hypothesis that the NIR intensities corresponded to the level of weathering since we have discovered that the natural patina of the stone was mostly invisible in the near-infrared spectrum and that the dominant deterioration pattern for both case studies was biological, while no physical damages were observable.

The first 3D mapping approach was to assume that the intensities were already a precise, detailed representation of the weathering levels. Although to increase interpretability, NIR textures were reduced to 3-bit grayscale. In this way, we created pseudo-mappings of the levels of weathering, which were then re-projected onto the final meshes.

For the second 3D mapping approach, after exhaustive tests to decide the optimal number of levels of deterioration that should be visualized, we classified the 3D NIR textured models according to 6 distinct classes/levels of weathering. The number of thematic mapping classes was selected to make more interpretable the distinguishably different levels of weathering between the case studies, and the not so distinct levels of weathering for each case study separately. The created thematic layers corresponded to levels of surface decay ranging from low -almost healthy material-, to very high -substantial surface biodeterioration and thicker deposits. To apply this type of mapping, we transferred the NIR information from the single-image textures to the triangles of the meshes and then used the colorized mesh to perform segmentation based on the color. Subsequently, we colored the respective 3D sub-models with different hues, and we measured the surface areas. For better visualization results, we also used artificial lighting according to the normals of the 3D meshes.

Results and discussion

Evaluation of metric results

In order to thoroughly assess the image-based modeling results, we recorded in detail their volumes, reconstruction errors, and processing durations for both software. We present the photogrammetric results in Table 2. We also evaluated the preservation of surface detail on the final 3D models and the levels of generated noise.

Table 2 Image-based reconstruction results

	Statue from the fountain of Hercules				Sculpture of Crist Crucified			
	VIS AMP	NIR AMP	VIS FZA	NIR FZA	VIS AMP	NIR AMP	VIS FZA	NIR FZA
Aligned images	180	180	176	180	142	142	70	140
Matching time	00:05:16	00:04:24	02:24:36	00:51:47	00:01:05	00:01:25	00:12:11	00:07:06
Alignment time	00:05:33	00:03:39	00:18:24	00:13:52	00:00:24	00:00:34	00:00:51	00:01:00
Tie points	454,192	426,852	258,384	177,250	89,440	53,780	35,861	42,321
Point projections	1,434,286	1,365,710	1,743,280	1,192,860	273,196	139,401	154,077	207,060
Reprojection errors	0.65	0.80	1.01	1.11	0.52	0.68	0.52	0.80
Densification time	01:43:36	02:17:14	02:06:24	03:09:11	00:23:10	00:24:13	00:55:20	02:31:58
Dense cloud points	14,676,050	15,719,040	5,580,119	4,916,655	2,058,186	2,033,498	4,210,383	4,343,056
Meshing time	00:08:35	00:09:07	00:05:23	00:03:50	00:01:23	00:01:34	00:02:30	00:05:40
Mesh vertices	5,000,615	5,000,615	3,693,700	3,244,014	2,424,234	2,355,906	2,312,486	2,316,916
Mesh triangles	10,000,000	10,000,000	7,375,384	6,473,051	4,845,581	4,707,857	4,604,754	4,623,336
Texturing time	00:10:29	00:10:43	00:24:37	00:13:20	00:09:25	00:06:05	00:18:25	00:08:57
Total processing time	02:13:29	02:45:07	05:19:24	04:32:00	00:35:27	00:33:51	01:29:17	02:54:41

We performed geometric comparisons amongst the models derived from different software and spectra, computing Hausdorff distances between the vertices of the final meshes. This task was executed in Cloud Compare with the Cloud-to-Cloud tool, after using an Iterative Closest Point (ICP) algorithm to perform fine registration. Additionally, we conducted comparisons with meshes produced with a STONEX F6 SR structured light scanner, which were down-sampled to match the density of the models produced with image-based techniques.

For the case study of the marble statue from the fountain of Hercules, image-based modeling resulted in full reconstructions of the object for both VIS and NIR datasets. Point clouds from both spectra were of similar volume, although FZA produced denser results than AMP. The re-projection errors of the reconstruction were also slightly higher for FZA. Despite the fact that the use of NIR images did not seem to influence the processing times, the NIR-produced meshes contained low levels of surface noise, concentrated at the areas where shadows could not be eliminated. It should be highlighted that NIR digitization resulted in the same level of surface detail preservation

as VIS digitization (see Fig. 3). Hausdorff distances between vertices of the final meshes for VIS and NIR reconstructions showed differences of 0.72 ± 0.58 mm for AMP and 0.73 ± 0.74 mm for FZA. In both cases, the differences with the mesh produced from the F6 SR scanner were in the range of 0.8 ± 0.7 mm. Textures were of the same quality. The NIR model finally selected for 3D mapping was the one from AMP because of the lower surface noise.

Fig. 3 Photogrammetric models, statue from the Fountain of Hercules (from left to right): AMP VIS, AMP NIR, FZA VIS, FZA NIR

For the case study of the stone sculpture of Crist Crucified, FZA was not able to reconstruct the object from all images for the VIS scenario (images from two out of four circular capturing patterns were oriented), but the problem was overcome with NIR imagery. However, this cannot be attributed to the different features visible on the NIR images, rather on the algorithmic implementations of the employed software. In this case, all the scenarios produced dense results of similar volume. Similar processing times were observed for VIS and NIR modeling, and similar to the last case study, slightly higher reconstruction errors. Furthermore, there was significant visible surface noise in both NIR models, but the level of surface detail preserved was identical as with VIS (see Fig. 4). Hausdorff distances between vertices of the final meshes for VIS and NIR reconstructions showed differences of

0.39 ± 0.25 mm for AMP and 0.29 ± 0.41 mm for FZA. Textures were of the same very high quality. The NIR mesh that was finally selected to apply 3D mapping was the one from AMP, because of the visibly lower surface noise. In both cases, the distances between the photogrammetric models and the meshes produced from the F6 SR scanner ranged bellow 0.70 mm.

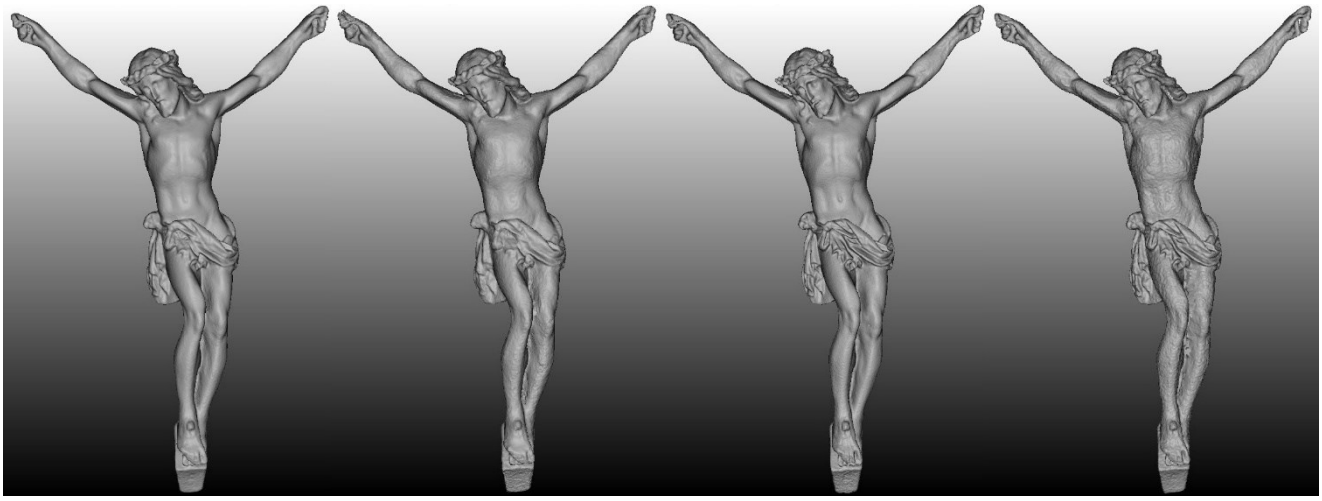

Fig. 4 Photogrammetric models, sculpture of Crist Crucified (from left to right): AMP VIS, AMP NIR, FZA VIS, FZA NIR

Evaluation of 3D mapping

As expected, the mapping results produced with the NIR models have a good correspondence with the real-life situation about the state of weathering. The suggested 3D image-based approaches are significantly more accurate than manual mapping by hand or by 2D CAD and GIS systems and allowed to map in three-dimensions details of up to sub-millimetric detail. They gave valuable first insight on the overall assessment of the surface weathering, which could not be achieved with a VIS textured model, because of the misinterpretations caused by the natural patina. The 3D segmentation performed on the models based on the NIR reflectance also allowed to record the area and percentage of each level of weathering and to compare the case studies involved (see Table 3).

Table 3 Areas of 3D surface weathering in comparison

Statue of Hercules			Sculpture of Christ	
Area (m^2)	Area (%)	Level of weathering (color)	Area (%)	Area (m^2)
0.048718	2.28	very-high (red)	0.00	0.000000
0.672628	31.41	high (orange)	0.00	0.000000
0.860497	40.19	medium-to-high (light orange)	1.15	0.003707
0.432027	20.18	medium (yellow)	5.27	0.017002
0.120743	5.64	medium-to-low (light green)	93.58	0.301840
0.006489	0.30	low (green)	0.00	0.000030

In the case of the application for the statue from the fountain of Hercules, and despite the problems created to 3D mapping by the remaining shadows at the occluded areas, we could easily distinguish the circular forms of the biodegradation patterns, in both protected and unprotected areas of the statue. Notably, significant weathering is present at shallow cavities and cracks whose origin is either due to the construction techniques or because of physical damage induced over time. Extensive high levels of deterioration are evident on almost the entire surface of the statue (see Fig. 5), as 73.88% of the surface was characterized by medium-to-high to very-high levels of deterioration according to our approach. Only 0.30 % was characterized by low levels of weathering. The observed high levels of bio-decay can be largely attributed to the characteristics of the external environment where the marble statue was positioned. The proximity of the sculpture to a water fountain, in combination with rain and moisture favors the action of biological agents, which was not the case for the second heritage object under study. For the first case study, the thematic 3D segmentation and visualization approach produced more comprehensive results than the direct use of the NIR reflectance values.

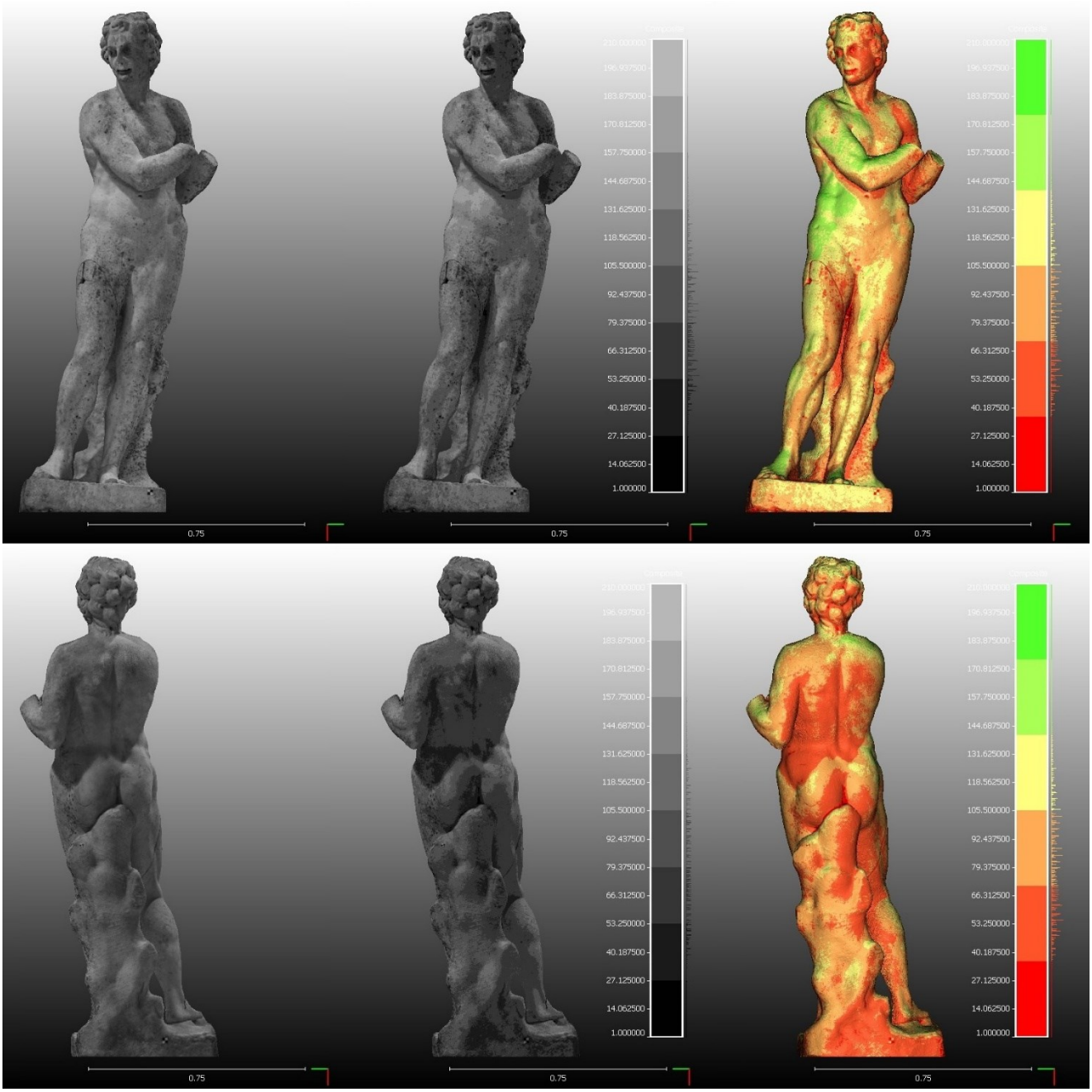

Fig. 5 Visualization of the levels of weathering for the statue of Hercules Fountain with high-resolution NIR texture (left), 3-bit NIR texture (center) and 3D thematic mapping after segmentation of the 3D model (right)

Unlike the previous example, 3D mapping after segmentation of the small sculpture of Christ Crucified showed relatively low levels of deterioration on the surface (see Fig. 6), as 93.58% of the total surface classified as medium-to-low or low deteriorated according to our approach. This result can be supported by the fact that the object was preserved in much better surrounding conditions that statue from the Fountain of Hercules that was long exposed to high moisture conditions. Only 5.27% of the total surface was classified as medium deteriorated and 1.15% as medium-to-high; these areas were concentrated on cavities around the hair, thorny wreath, and chest. For this

case study, the visualization with the reduced NIR texture provided more comprehensive results towards the assessment of the state of preservation.

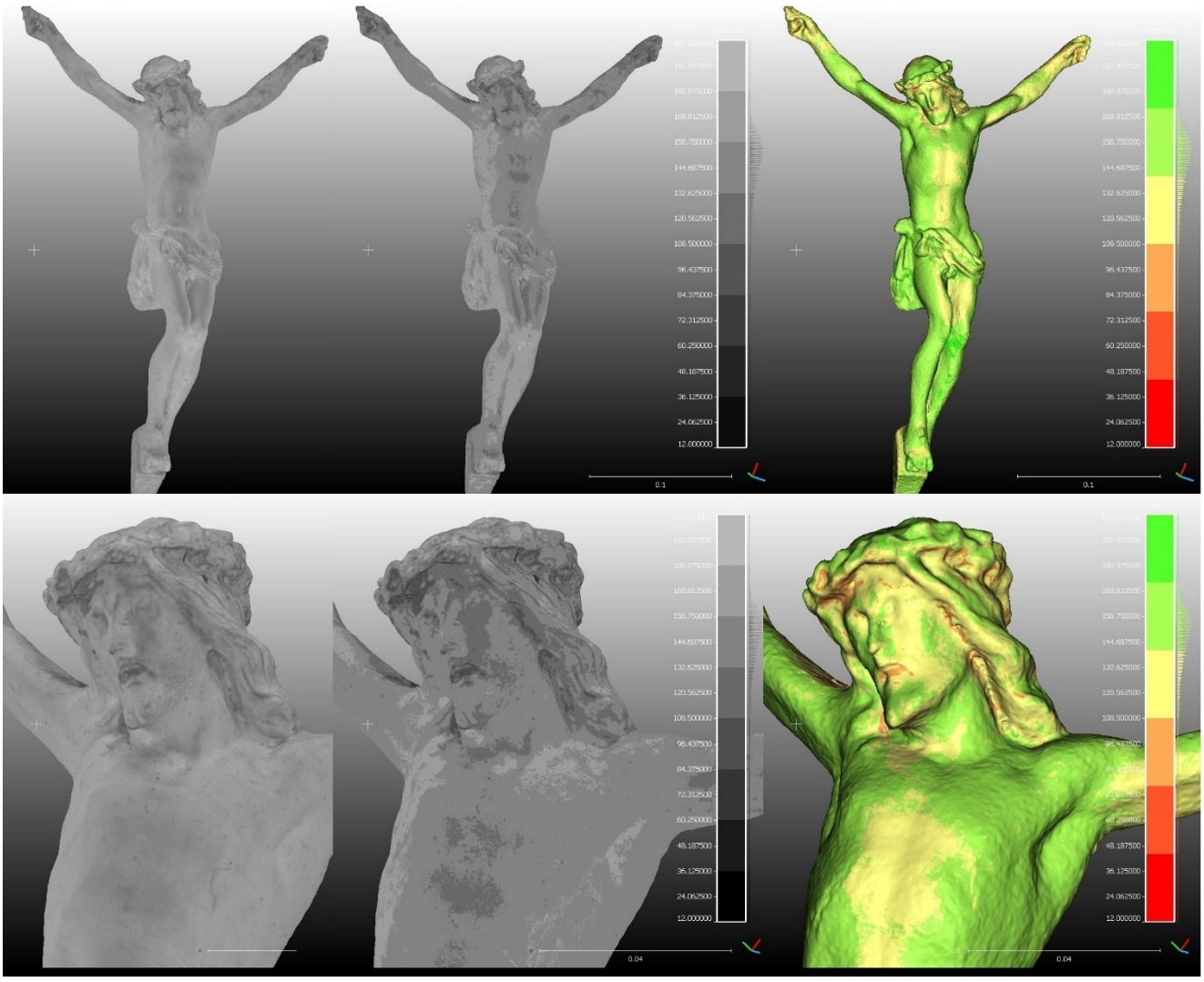

Fig. 6 Visualization of the levels of weathering for the sculpture of Christ Crucified with high-resolution NIR texture (left), 3-bit NIR texture (center) and 3D thematic mapping after segmentation of the 3D model (right)

Conclusions

This paper presented a novel approach aimed towards mapping the levels of weathering for historical objects, combining contemporary image-based 3D reconstruction software, near-infrared imaging from a modified camera, and 3D mapping techniques. In this work, we constructed high-resolution 3D models of stone sculptures from near-infrared imagery and proved their metric validity by performing extensive comparisons with models from visible imagery. Then we evaluated the capacity of the most detailed near-infrared models to be used for evaluating the state of preservation of the historical surfaces proving the feasibility of the combined approach. The suggested

approach has the advantages of being low-cost, rapid, easy to implement and adjustable for different cases of heritage applications, comparing to traditional methods for manual decay mapping. It has the additional advantage of combining the thematic information produced with the three-dimensional topology of the object, making possible accurate measurements and planning of further scientific investigations and conservation interventions. The investigated method cannot replace extensive diagnostical investigations but can support them in order to reduce times and costs.

Regarding the metric aspect of the study, we should underline that Metashape Professional generally provided less noisy meshes from the near-infrared datasets than Zephyr Aerial and resulted in slightly smaller statistical reconstruction errors. Although results from both software were practically identical for conservation studies of millimeter accuracy, even considering the metric results produced with visible imagery. As for the 3D mapping results, we observed that reducing the information on the near-infrared textures gave a significant boost in the observation of different levels of weathering. Even more, carefully selecting the number of the levels of decay that should be visualized for an accurate representation of the pathology and segmenting the models according to near-infrared reflectance to produce thematic 3D mapping results, enhanced the ability to interpret the deterioration patterns and enabled measurement for each segmented part of the surface. To conclude, the method suggested here shows high potential, and therefore the authors would like to express their interest in evaluating it for architectural heritage combined with thermal imaging and for other typologies of tangible heritage, which also are susceptible to different types of decay.

Declarations

Funding

This project has received funding from the European Union's Framework Program for Research and Innovation Horizon 2020 (2014–2020) under the Marie-Skłodowska Curie Grant Agreement No. 754511 and from the Compagnia di San Paolo.

Competing interests

The authors declare no conflict of interest. The funders had no role in the design of the study; in the collection, analyses, or interpretation of data; in the writing of the manuscript, or in the decision to publish the results.

Availability of data and materials

The datasets used and/or analyzed during the current study are available from the corresponding author on reasonable request.

Author contributions

Conceptualization: Efstathios Adamopoulos; Data curation: Efstathios Adamopoulos; Methodology: Efstathios Adamopoulos; Validation: Efstathios Adamopoulos and Fulvio Rinaudo; Formal analysis: Efstathios Adamopoulos; Investigation: Efstathios Adamopoulos; Resources: Efstathios Adamopoulos and Fulvio Rinaudo; Software: Efstathios Adamopoulos; Writing - original draft preparation: Efstathios Adamopoulos; Writing - review & editing: Efstathios Adamopoulos and Fulvio Rinaudo; Visualization: Efstathios Adamopoulos; Supervision: Fulvio Rinaudo; Project administration: Fulvio Rinaudo; Funding acquisition: Fulvio Rinaudo.

References

Adamopoulos E, Rinaudo F (2019) An Updated Comparison on Contemporary Approaches for Digitization of Heritage Objects. In: Catelani M, Daponte P (eds). Proceedings of the 5th IMEKO TC-4 International Conference on Metrology for Archaeology and Cultural Heritage, Florence, Italy, 4th–6th December 2019

Adamopoulos E, Rinaudo F (2020) Enhancing Image-Based Multiscale Heritage Recording with Near-Infrared Data. ISPRS Int. J. Geo-Inf. 9(4):269. https://doi.org/10.3390/ijgi9040269

Adamopoulos E, Rinaudo F, Bovero A (2019) First assessments on heritage science oriented image-based modeling using low-cost modified and mobile cameras. Int Arch Photogramm Remote Sens Spatial Inf Sci XLII-2/W17:23–30. https://doi.org/10.5194/isprs-archives-XLII-2-W17-23-2019

Adamopoulos E, Tsilimantou E, Keramidas V, et al (2017) Multi-sensor documentation of metric and qualitative information of historic stone structures. ISPRS Ann Photogramm Remote Sens Spatial Inf Sci IV-2/W2:1–8. https://doi.org/10.5194/isprs-annals-IV-2-W2-1-2017

Ansel J, Gerling C, Hofmeister S, Schick S (2016) Zwei Heiligenfiguren aus der katholischen Marienkirche in Bad Mergentheim. Ein außergewöhnliches Restaurierungsprojekt und der Testlauf für eine 3-D-Dokumentation. Denkmalpflege in Baden-Württemberg–Nachrichtenblatt der Landesdenkmalpflege 45(3):157-163.

Apollonio FI, Basilissi V, Callieri M, et al (2018) A 3D-centered information system for the documentation of a complex restoration intervention. J Cult Herit 29:89–99. https://doi.org/10.1016/j.culher.2017.07.010

Callieri M, Ranzuglia G, Dellepiane M, et al (2013) Meshlab as a Complete Open Tool for the Integration of Photos and Colour with High-Resolution 3D Geometry Data. In: Graeme E, Sly T, Chrysanthi A, Murrieta-Flores P, Papadopoulos C, Romanowska I, Wheatley D, (eds) Archaeology in the Digital Era Volume 2. Proceedings of the 40th Conference on Computer Applications and Quantitative Methods in Archaeology, Southampton, United Kingdom, 26th–30th March 2012

Campanaro DM, Landeschi G, Dell'Unto N, Leander Touati A-M (2016) 3D GIS for cultural heritage restoration: A 'white box' workflow. J Cult Herit 18:321–332. https://doi.org/10.1016/j.culher.2015.09.006

Catelli E, Randeberg L, Strandberg H, et al (2018) Can hyperspectral imaging be used to map corrosion products on outdoor bronze sculptures? J Spectral Imaging 7:a10. https://doi.org/10.1255/jsi.2018.a10

Chen S, Yang H, Wang S, Hu Q (2018) Surveying and Digital Restoration of Towering Architectural Heritage in Harsh Environments: a Case Study of the Millennium Ancient Watchtower in Tibet. Sustainability 10:3138. https://doi.org/10.3390/su10093138

Chrysostomou CZ, Hadjimitsis DG, Agapiou A, et al (2010) Application of non-destructive techniques in assessing the quality of stone building materials in cultural heritage structures in Cyprus: Use of ultrasonic and 3D laser scanning integrated approach for diagnostic tests. In: Euromed2010: Digital Heritage Short Papers. Ioannides M, Fellner D, Georgopoulos A, Hadjimitsis D, (eds). Proceedings of the 3rd International Euro-Mediterranean Conference dedicated on Digital Heritage, Limassol, Cyprus, 8th–13th November 2010

Columbu S, Verdiani G (2014) Digital Survey and Material Analysis Strategies for Documenting, Monitoring and Study the Romanesque Churches in Sardinia, Italy. In: Ioannides M, Magnenat-Thalmann N, Fink E, et al. (eds) Digital Heritage. Progress in Cultural Heritage: Documentation, Preservation, and Protection. Springer International Publishing, Cham, pp 446–453

Delaney JK, Thoury M, Zeibel JG, et al (2016) Visible and infrared imaging spectroscopy of paintings and improved reflectography. Herit Sci 4:6. https://doi.org/10.1186/s40494-016-0075-4

Delegou ET, Tsilimantou E, Oikonomopoulou E, et al (2013) Mapping of Building Materials and Conservation Interventions Using GIS: The Case of Sarantapicho Acropolis and Erimokastro Acropolis in Rhodes. Int J of Heritage in the Digital Era 2:631–653. https://doi.org/10.1260/2047-4970.2.4.631

Douglass M, Lin S, Chodoronek M (2015) The Application of 3D Photogrammetry for In-Field Documentation of Archaeological Features. Adv archaeol pract 3:136–152. https://doi.org/10.7183/2326-3768.3.2.136

Dumas F, Giamello M, Guasparri G, Meccheri M, Mugnaini S, Sabatini G, Scala A, (2004) The meaning of the taroli on the marble surface of Michelangelo's David. In: Bracci S, Falletti F, Matteini M, Scopigno R, (eds) Exploring David. Diagnostic Tests and State of Conservation. Giunti: Florence, pp 136–138

Fazio L, Lo Brutto M (2020) 3D survey for the archaeological study and virtual reconstruction of the “Sanctuary of Isis” in the ancient Lilybaeum (Italy). Virtual archaeol rev 11:1. https://doi.org/10.4995/var.2020.11928

Fitzner B (2002) Damage diagnosis on stone monuments-in situ investigation and laboratory studies. In: Proceedings of the International Symposium of the Conservation of the Bangudae Petroglyph, Ulsan City, South Korea, 15th July 2002

Fitzner B (2004) Documentation and evaluation of stone damage on monuments. In: Kwiatkowski D, Löfvendahl R, (eds) Proceedings of the 10th International Congress on Deterioration and Conservation of Stone, Stockholm, Sweden, 27th June–2nd July 2004

Fonstad MA, Dietrich JT, Courville BC, et al (2013) Topographic structure from motion: a new development in photogrammetric measurement. Earth Surf Process Landforms 38:421–430. https://doi.org/10.1002/esp.3366

Gasanova S, Pagès-Camagna S, Andrioti M, Hermon S (2018) Non-destructive in situ analysis of polychromy on ancient Cypriot sculptures. Archaeol Anthropol Sci 10:83–95. https://doi.org/10.1007/s12520-016-0340-1

Georgopoulos A, Stathopoulou EK (2017) Data Acquisition for 3D Geometric Recording: State of the Art and Recent Innovations. In: Vincent ML, López-Menchero Bendicho VM, Ioannides M, Levy TE (eds) Heritage and Archaeology in the Digital Age. Springer International Publishing, Cham, pp 1–26

Girelli VA, Tini MA, Dellapasqua M, Bitelli G (2019) High resolution 3D acquisition and modelling in cultural heritage knowledge and restoration projects: The survey of the fountain of Neptune in Bologna. Int Arch Photogramm Remote Sens Spatial Inf Sci XLII-2/W11:573–578. https://doi.org/10.5194/isprs-archives-XLII-2-W11-573-2019

Hassani F (2015) Documentation of cultural heritage; techniques, potentials, and constraints. Int Arch Photogramm Remote Sens Spatial Inf Sci XL-5/W7:207–214. https://doi.org/10.5194/isprsarchives-XL-5-W7-207-2015

Inkpen RJ, Fontana D, Collier P (2001) Mapping decay: integrating scales of weathering within a GIS. Earth Surf Process Landforms 26:885–900. https://doi.org/10.1002/esp.234

Kioussi A, Karoglou M, Labropoulos K, et al (2013) Integrated documentation protocols enabling decision making in cultural heritage protection. J Cult Herit 14:e141–e146. https://doi.org/10.1016/j.culher.2013.01.007

Koehl M, Fuchs M (2019) 3D Modelling of architectural blocks and antique sculptures for the experiments and the promotion of archaeological heritage – experiments in Alsace. Int Arch Photogramm Remote Sens Spatial Inf Sci XLII-2/W15:625–632. https://doi.org/10.5194/isprs-archives-XLII-2-W15-625-2019

Koutsoudis A, Vidmar B, Ioannakis G, et al (2014) Multi-image 3D reconstruction data evaluation. J Cult Herit 15:73–79. https://doi.org/10.1016/j.culher.2012.12.003

Kozub B, Kozub P (2016) 3D Photo monitoring as a long-term monument mapping method for stone sculptures. In: Science and Art: A Future for Stone. Hughes J, Howind T, (eds) Proceedings of the 13th International Congress on the Deterioration and Conservation of Stone Volume 2, Glasgow, Scotland, 6th–10th September 2016

Lerma JL, Cabrelles M, Akasheh TS, Haddad NA (2012) Documentation of Weathered Architectural Heritage with Visible, near Infrared, Thermal and Laser Scanning Data. Int J of Heritage in the Digital Era 1:251–275. https://doi.org/10.1260/2047-4970.1.2.251

Lerma JL, Ruiz LÁ, Buchón F (2000) Application of spectral and textural classifications to recognize materials and damages on historic building facades. Int. Arch. Photogramm. Remote Sens. Spatial Inf. Sci. XXXIII-B5: 480–483

López JAB, Jiménez GA, Romero MS, et al (2016) 3D modelling in archaeology: The application of Structure from Motion methods to the study of the megalithic necropolis of Panoria (Granada, Spain). J Archaeol Sci Rep 10:495–506. https://doi.org/10.1016/j.jasrep.2016.11.022

Malik US, Guidi G (2018) Massive 3D digitization of sculptures: Methodological approaches for improving efficiency. IOP Conf Ser: Mater Sci Eng 364:012015. https://doi.org/10.1088/1757-899X/364/1/012015

Mandelli A, Achille C, Tommasi C, Fassi F (2017) Integration of 3D models and diagnostic analyses through a conservation-oriented information system. Int Arch Photogramm Remote Sens Spatial Inf Sci XLII-2/W5:497–504. https://doi.org/10.5194/isprs-archives-XLII-2-W5-497-2017

Marvasi M, Donnarumma F, Frandi A, et al (2012) Black microcolonial fungi as deteriogens of two famous marble statues in Florence, Italy. Int Biodeterior Biodegradation 68:36–44. https://doi.org/10.1016/j.ibiod.2011.10.011

Mascalchi M, Osticioli I, Cuzman OA, et al Diagnostic campaign and innovative conservation treatments carried out on the statue “La Speranza” by Odoardo Fantacchiotti. In: Calcagnile L, Daponte P, (eds) Proceedings of

the 3rd IMEKO TC-4 International Conference on Metrology for Archaeology and Cultural Heritage, Lecce, Italy, 23th–25th October 2017

McCabe S, Smith BJ, Warke PA (2007) An holistic approach to the assessment of stone decay: Bonamargy Friary, Northern Ireland. Geological Society, London, Special Publications 271:77–86. https://doi.org/10.1144/GSL.SP.2007.271.01.09

McCarthy J (2014) Multi-image photogrammetry as a practical tool for cultural heritage survey and community engagement. J Archaeol Sci 43:175–185. https://doi.org/10.1016/j.jas.2014.01.010

Moropoulou A, Labropoulos K, Delegou ET, et al (2013) Non-destructive techniques as a tool for the protection of built cultural heritage. Constr Build Mater 48:1222–1239. https://doi.org/10.1016/j.conbuildmat.2013.03.044

Nascimbene J, Salvadori O (2008) Lichen recolonization on restored calcareous statues of three Venetian villas. Int Biodeterior Biodegradation 62:313–318. https://doi.org/10.1016/j.ibiod.2007.11.005

Ortiz R, Ortiz P, Vázquez MA, Martín JM (2017) Integration of georeferenced informed system and digital image analysis to assess the effect of cars pollution on historical buildings. Constr Build Mater 139:320–333. https://doi.org/10.1016/j.conbuildmat.2017.02.030

Pfeuffer C, Rahrig M, Snethlage R, Drewello R (2018) 3D mapping as a tool for the planning of preservation measures on sculptures made of natural stone. Environ Earth Sci 77:312. https://doi.org/10.1007/s12665-018-7479-2

Pronti L, Romani M, Verona-Rinati G, et al (2019) Post-Processing of VIS, NIR, and SWIR Multispectral Images of Paintings. New Discovery on the The Drunkenness of Noah, painted by Andrea Sacchi, Stored at Palazzo Chigi (Ariccia, Rome). Heritage 2:2275–2286. https://doi.org/10.3390/heritage2030139

Russo M, Carnevali L, Russo V, et al (2019) Modeling and deterioration mapping of façades in historical urban context by close-range ultra-lightweight UAVs photogrammetry. Int J Archit Herit 13:549–568. https://doi.org/10.1080/15583058.2018.1440030

Salonia P, Negri A (2003) Historical buildings and their decay: Data recording, analysis and transferring in an ITC environment. Int. Arch. Photogramm. Remote Sens. Spatial Inf. Sci. XXXIV-5/W12:302–306

Santos P, Ritz M, Fuhrmann C, Fellner D (2017) 3D mass digitization: a milestone for archeological documentation. Virtual archaeol rev 8:1. https://doi.org/10.4995/var.2017.6321

Sfarra S, Ibarra-Castanedo C, Ridolfi S, et al (2014) Holographic Interferometry (HI), Infrared Vision and X-Ray Fluorescence (XRF) spectroscopy for the assessment of painted wooden statues: a new integrated approach. Appl Phys A 115:1041–1056. https://doi.org/10.1007/s00339-013-7939-1

Siedler G, Vetter S (2013) Modern methods of documentation for conservation - digital mapping in metigo® MAP, Software for documentation, mapping and quantity survey and analysis. In: Rogerio-Candelera MA, Lazzari M, Cano E, (eds) Science and Technology for the Conservation of Cultural Heritage. Taylor & Francis Group, London, pp 163–168

Suchocki C (2020) Comparison of Time-of-Flight and Phase-Shift TLS Intensity Data for the Diagnostics Measurements of Buildings. Materials 13:353. https://doi.org/10.3390/ma13020353

Tiano P (2002) Biodegradation of Cultural Heritage: Decay Mechanisms and Control Methods. Seminar article, New University of Lisbon

Toprak AS, Polat N, Uysal M (2019) 3D modeling of lion tombstones with UAV photogrammetry: a case study in ancient Phrygia (Turkey). Archaeol Anthropol Sci 11:1973–1976. https://doi.org/10.1007/s12520-018-0649-z

Tucci G, Bonora V, Conti A, Fiorini L (2015) Benchmarking Range-Based and Image-Based Techniques for Digitizing a Glazed Earthenware Frieze. ISPRS Ann Photogramm Remote Sens Spatial Inf Sci II-5/W3:315–322. https://doi.org/10.5194/isprsannals-II-5-W3-315-2015

Tucci G, Bonora V, Conti A, Fiorini L (2017) High-quality 3D models and their use in a cultural heritage conservation project. Int Arch Photogramm Remote Sens Spatial Inf Sci XLII-2/W5:687–693. https://doi.org/10.5194/isprs-archives-XLII-2-W5-687-2017

Vandivere A, van Loon A, Dooley KA, et al (2019) Revealing the painterly technique beneath the surface of Vermeer's Girl with a Pearl Earring using macro- and microscale imaging. Herit Sci 7:64. https://doi.org/10.1186/s40494-019-0308-4

Vázquez MA, Galán E, Guerrero MA, Ortiz P (2011) Digital image processing of weathered stone caused by efflorescences: A tool for mapping and evaluation of stone decay. Constr Build Mater 25:1603–1611. https://doi.org/10.1016/j.conbuildmat.2010.10.003

Webb EK, Robson S, MacDonald L, et al (2018) Spectral and 3D cultural heritage documentation using a modified camera. Int Arch Photogramm Remote Sens Spatial Inf Sci XLII–2:1183–1190. https://doi.org/10.5194/isprs-archives-XLII-2-1183-2018